ACS Combinatorial Science

pubs.acs.org/acscombsci

Letter

(Hetero-)(arylidene)arylhydrazides as Multitarget-Directed Monoamine Oxidase Inhibitors

Ashique Palakkathondi,[#] Jong Min Oh,[#] Sanal Dev,[#] T. M. Rangarajan, Swafvan Kaipakasseri, Fathima Sahla Kavully, Nicola Gambacorta, Orazio Nicolotti, Hoon Kim,* and Bijo Mathew*

Cite This: https://dx.doi.org/10.1021/acscombsci.0c00136

Read Online

ABSTRACT: Fourteen (hetero-)(arylidene)arylhydrazide derivatives (**ABH1−ABH14**) were synthesized, and their inhibitory activities against monoamine oxidases (MAOs) and acetylcholinesterase (AChE) were evaluated. Compound **ABH5** most potently inhibited MAO-B with an IC_{50} value of 0.025 ± 0.0019 μM; **ABH2** and **ABH3** exhibited high IC_{50} values as well. Most of the compounds weakly inhibited MAO-A, except **ABH5** (IC_{50} = 3.31 ± 0.41 μM). Among the active compounds, **ABH2** showed the highest selectivity index (SI) of 174 for MAO-B, followed by **ABH5** (SI = 132). **ABH3** and **ABH5** effectively inhibited AChE with IC_{50} values of 15.7 ± 6.52 and 16.5 ± 7.29 μM, respectively, whereas the other compounds were weak inhibitors of AChE. **ABH5** was shown to be a reversible competitive inhibitor for MAO-A and MAO-B with K_i values of 0.96 ± 0.19 and 0.024 ± 0.0077 μM, respectively, suggesting that this molecule can be considered as an interesting candidate for further development as a multitarget inhibitor relating to neurodegenerative disorders.

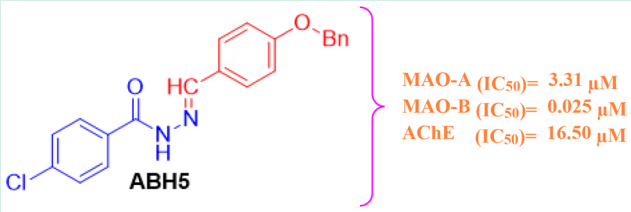

KEYWORDS: *(Hetero-)(arylidene)arylhydrazide, MAOs, AChE, Kinetics, Docking analysis, Multitarget inhibitor*

Alzheimer's disease (AD) is the most prevalent age-related neurodegenerative disorder characterized by the impairment of cognitive functions that leads to memory deficit.[1] Molecular signatures of AD include the deposition of β-amyloid plaques, increase in free radical-based oxidative stress, and diminished levels of acetylcholine.[2] Several lines of evidence concerned with the multifactorial pathogenesis of AD suggest that the conventional "one drug-one target" concept does not always guarantee for the success in AD treatment.[3] For example, disregulated levels of the enzyme monoamine oxidase-B (MAO-B) in brain cells leads to excessive production of hydrogen peroxide responsible for cellular degeneration in AD patients and aging of the brain.[4] Recent *in vivo* two-photon imaging studies showed a clear evidence for elevated MAO-B enzyme activity around amyloid β-plaques in aged AD mice.[5] This finding suggests that the progress of age-related AD may also be associated with increased levels of MAO-B activity.

A new class of MAO-B inhibitors comprised of two aryl or heteroaryl rings connected through a short spacer have recently been described.[6] Such spacers as α,β-unsaturated ketones,[7−13] pyrazoline,[14] hydrazones,[15,16] and anilide/enamides[17,18] have received attention (Figure 1). Here we describe an expansion of this theme to 14 (hetero-)(arylidene)arylhydrazides, with an investigation of their inhibitory activity toward two forms of MAO and acetylcholinesterase (AChE). The most potent compound identified in these *in vitro* tests was further analyzed by molecular docking to identify potential interactions at the binding sites of MAO-B and AChE.

Compounds **ABH1−ABH14** were prepared by the straightforward condensation of corresponding hydrazides and aldehydes in moderate yields (51−74%, Table 1).[19] Six compounds (**ABH1−ABH6**) were derived from 4-chlorobenzohydrazide and eight compounds (**ABH7−ABH14**) were derived from isonicotinohydrazide.

The 14 compounds were tested for their MAOs and AChE inhibitory potencies by literature methods,[20,21] using toloxatone and clorgyline as positive controls for MAO-A, lazabemide and pargyline for MAO-B, and tacrine for AChE (Table 2). Recombinant human MAO-A and MAO-B were employed, with kynuramine (0.06 mM = 1.7 × K_m) and benzylamine (0.3 mM = 2 × K_m) as substrates, respectively. Compounds **ABH1−ABH6** showed potent inhibitory activity against MAO-B with residual activities of <35% at 10 μM concentration, except **ABH4** (71.3%). **ABH5** was found to have the highest inhibitory activity against MAO-B with an IC_{50} of 0.025 μM, followed by **ABH2** and **ABH3** (IC_{50} = 0.23 and 0.58 μM, respectively) (Table 2). In contrast, eight compounds (**ABH7−ABH14**) derived from isonicotinohydrazide had weak inhibitory activities against MAO-B with residual activities of > ∼ 40% at 10 μM, and

Received: July 8, 2020
Revised: September 28, 2020

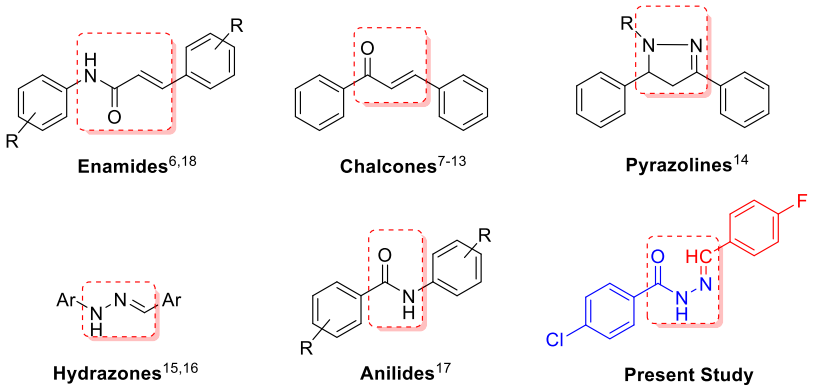

Figure 1. Small molecules with two aryl groups connected through various spacers for MAOs inhibitory activities.

Table 1. Synthesis of (Hetero)arylidenebenzohydrazides

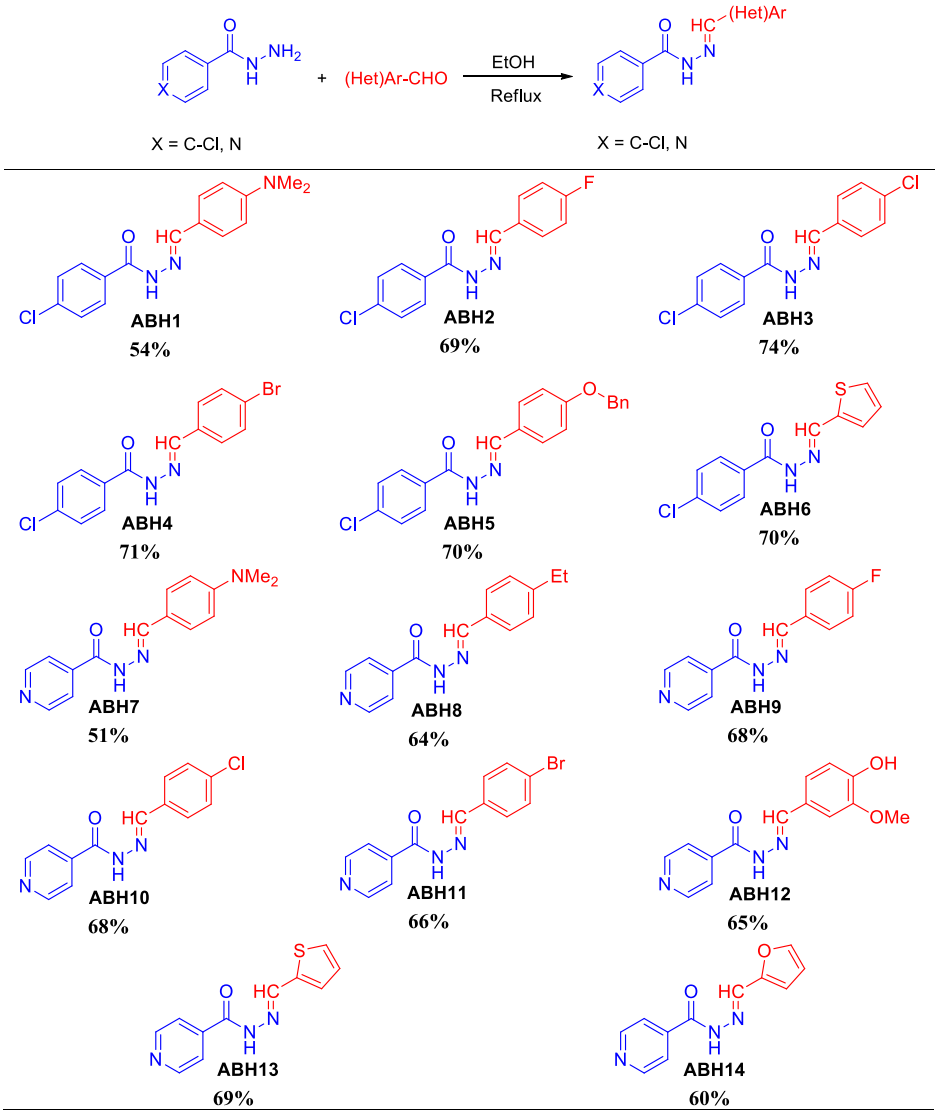

hence IC_{50} values were >10 μM, except for **ABH8** (IC_{50} = 8.38 μM).

In contrast, most of these compounds (both aryl and heteroarylhydrazide) weakly inhibited MAO-A, except **ABH5** (residual activity = 15.4% at 10 μM; IC_{50} = 3.31 μM), followed by **ABH10**, **ABH11**, and **ABH8** (IC_{50} = 13.6, 14.2, and 32.1 μM, respectively) (Table 2). Interestingly, **ABH5** had significant activities toward MAO-A and MAO-B with a high SI of 132 for MAO-B, and **ABH2** showed the highest SI of 174 for MAO-B. On the other hand, all compounds weakly inhibited AChE with >70% of residual activities at 10 μM. **ABH3** and **ABH5** effectively inhibited AChE with IC_{50} values of 15.7 and 16.5 μM,

https://dx.doi.org/10.1021/acscombsci.0c00136
ACS Comb. Sci. XXXX, XXX, XXX−XXX

Table 2. Inhibitions of Recombinant Human MAO Enzymes and AChE by Acylhydrazone Derivatives[a]

compounds	residual activity (%) at 10 μM			IC_{50} (μM)			SI[b]
	MAO-A	MAO-B	AChE	MAO-A	MAO-B	AChE	
ABH1	82.6 ± 5.89	27.5 ± 2.05	75.4 ± 1.69	>40	7.69 ± 0.71	–	>5.20
ABH2	98.9 ± 0.54	19.7 ± 2.38	70.2 ± 6.73	>40	0.23 ± 0.021	–	>173.9
ABH3	87.5 ± 0.98	31.2 ± 1.02	65.9 ± 5.93	>40	0.58 ± 0.16	15.7 ± 6.52	>69.0
ABH4	90.6 ± 1.47	71.3 ± 1.02	71.3 ± 5.93	>40	>40	–	–
ABH5	15.4 ± 2.08	−2.14 ± 0.60	67.2 ± 7.31	3.31 ± 0.41	0.025 ± 0.0019	16.5 ± 7.29	132.4
ABH6	92.0 ± 1.62	32.0 ± 2.38	71.4 ± 4.21	>40	4.36 ± 0.36	–	>9.17
ABH7	93.1 ± 1.54	79.6 ± 4.12	75.6 ± 1.57	>40	>40	–	–
ABH8	76.1 ± 0.00	39.9 ± 3.10	99.5 ± 0.24	32.1 ± 1.55	8.38 ± 2.91	–	3.83
ABH9	91.5 ± 3.98	87.7 ± 6.20	98.8 ± 0.71	>40	>40	–	–
ABH10	47.8 ± 2.05	51.5 ± 1.37	71.7 ± 3.93	13.6 ± 0.97	12.4 ± 1.00	–	1.10
ABH11	65.3 ± 2.70	54.5 ± 5.56	74.7 ± 0.42	14.2 ± 0.97	18.7 ± 3.89	–	0.76
ABH12	87.3 ± 9.96	95.2 ± 0.62	98.8 ± 0.71	>40	>40	–	–
ABH13	90.9 ± 4.61	86.4 ± 5.49	85.0 ± 3.93	>40	>40	–	–
ABH14	97.4 ± 0.52	95.3 ± 3.02	96.6 ± 9.75	>40	>40	–	–
toloxatone	–	–	–	1.08 ± 0.025	–	–	–
clorgyline	–	–	–	0.0070 ± 0.00070	–	–	–
lazabemide	–	–	–	–	0.11 ± 0.016	–	–
pargyline	–	–	–	–	0.11 ± 0.0047	–	–
tacrine	–	–	–	–	–	0.12 ± 0.0074	–

[a]Results are expressed as the means ± standard errors of duplicate experiments. Values for reference compounds were determined after preincubation for 30 min with enzyme. [b]SI values are expressed for MAO-B as compared with MAO-A.

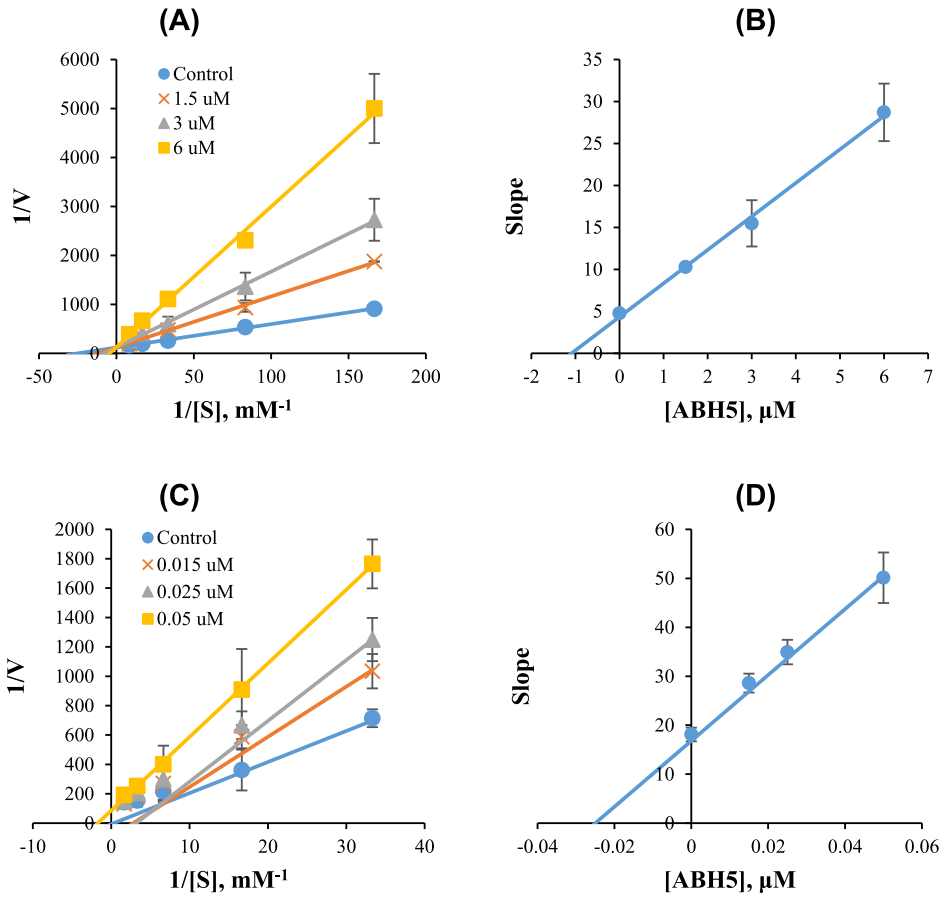

Figure 2. Lineweaver−Burk plots for MAO-A (A) and MAO-B (C) inhibitions by **ABH5** and respective secondary plots (B and D) of the slopes vs inhibitor concentrations.

respectively (Table 2). Collectively, **ABH5** is possessed a significant inhibitory profile toward all three enzymes, MAO-A, MAO-B, and AChE, and thus making it open to address the rational design of novel multitarget inhibitors.

https://dx.doi.org/10.1021/acscombsci.0c00136
ACS Comb. Sci. XXXX, XXX, XXX−XXX

Structure−activity relationship of these compounds can be described as two parts viz the compounds bearing 4-chloroaryl part (series 1) and pyridyl part (series 2). Interstingly, series 1 compounds were significantly active toward MAO-B inhibition compared to series 2 compounds. However, only few derivaties of both series showed moderate inhibitions toward MAO-A and AChE. None of the compounds of series 2 were active toward AChE inhibition. Considering MAO-B, the series 1 compounds, **ABH1**−**ABH3**, **ABH5**, and **ABH6**, with the benzylidene moiety bearing the substituents such as -NMe_2, -F, -Cl, benzyloxy, and thiophenyl, respectively, showed effective inhibitory activities, whereas the series 2 compounds (**ABH7**, **ABH9**, and **ABH12**−**ABH14**) showed weak inhibition. Among the substituents studied, benzyloxy group (**ABH5**) showed the greatest inhibitory effect. Therefore, 4-chloroaryl part (series 1) can be considered as a good pharmacophore unit for MAO-B inhibition rather than pyridyl part. Considering MAO-A, the only compound **ABH5** of series 1 showed effective inhibitory effect, suggesting that the benzyloxy substituent effectively interacts with MAO-A. However, **ABH8**, **ABH10**, and **ABH11** of series 2 showed moderate inhibitory activities, also suggesting that pyridyl part can be an effective pharmacophore unit for MAO-A inhibition. In contrast, none of all the compounds were not effective toward AChE inhibition, except **ABH5** and **ABH3**. Therefore, no substituents and parts might effectively intereact with AChE.

Kinetics experiments were conducted at five substrate concentrations and inhibition studies were at three inhibitor concentrations, that, ∼ $1/2 \times IC_{50}$, IC_{50}, and $2 \times IC_{50}$. K_i value and inhibitor type were determined by using Lineweaver−Burk (LB) plot and secondary plot.[22] Kinetics studies of **ABH5** were performed on MAO-A and MAO-B inhibitions. LB plots and secondary plots showed that **ABH5** was a competitive inhibitor for MAO-A and MAO-B (Figure 2A and C), with K_i values of 0.96 ± 0.19 and 0.024 ± 0.0077 μM, respectively (Figure 2B and D). These results suggest that **ABH5** binds to the active site of free enzyme by competing with the substrate and is potent, selective, and competitive inhibitor for MAO-A and MAO-B.

The reversibility study was determined by dialysis method.[23] Dialysis experiments were performed by reacting MAO-B and the inhibitor or reference inhibitors at approximately twice of the IC_{50} in 0.1 M sodium phosphate buffer for 30 min and dialyzed for 6 h with a buffer change. Residual activities were calculated for undialyzed (A_U) and dialyzed (A_D) experiments compared to controls (i.e., without inhibitor). Reversibility studies on MAO-A and MAO-B inhibitions were conducted for **ABH5**, the most potent compound. The inhibition of MAO-A by **ABH5** was recovered from 38.4 (value of A_U) to 85.9% (value of A_D). The recovery value was similar to that of the reversible reference toloxatone, from 38.0 to 83.7% and higher than that of the irreversible reference clorgyline (recovery from 29.2 to 32.0%). For MAO-B, inhibition by **ABH5** was recovered from 35.6 to 80.0%. The recovery value was similar to that of the reversible reference lazabemide, from 27.4 to 86.9% and higher than that of the irreversible reference pargyline (recovery from 24.8 to 35.1%). These experiments showed that inhibitions of MAO-A and MAO-B by **ABH5** were recovered to the reversible reference levels, suggesting the compound played as a reversible inhibitor (Figure 3).

Structure-based studies were employed to analyze the binding modes of **ABH2**, **ABH3**, and **ABH5** toward MAO-A, MAO-B, and AChE, whose X-ray solved structures were taken from the Protein Data Bank (PDB) with the entries 2Z5X, 2V5Z, and

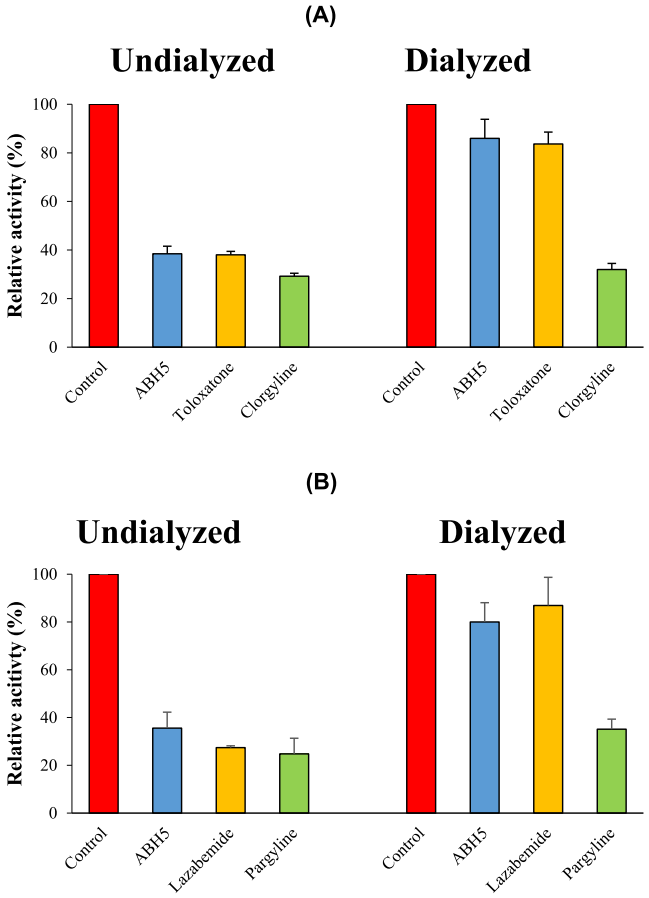

Figure 3. Recovery of MAO-A (A) and MAO-B (B) inhibitions by **ABH5**, using dialysis experiments.

4EY7, respectively. With the purpose of inspecting their multitarget activity,[24−26] the enzymes were processed using the protein preparation wizard available from the Schrödinger suite:[27,28] this step allows to refine and optimize the crystal structures, correcting the protonation states and carrying out energy minimization. In this respect, nine water molecules within MAO-A and eight water molecules within MAO-B were kept and not deleted.[29] Next, the ligand structures to be docked were prepared using the LigPrep tool[30] that allows generating the ionization state at physiological pH as well as all the possible tautomers. The obtained files were, thus, used for docking simulations by employing Grid-based Ligand Docking with Energetics (GLIDE).[31] The enclosing box was centered on the cognate ligand center of mass of the three PDB structures, with an edge of 10 Å × 10 Å × 10 Å and 28 Å × 28 Å × 28 Å for the inner and outer boxes, respectively. The default force Field OPLS_2005[32] and standard Precision (SP) docking protocol with default settings were employed for docking simulations. To corroborate the validity of docking studies, redocking simulations were performed on the cognate ligands in their binding sites. Cognate ligands HRM, SAG, and Donepezil for MAO-A, MAO-B, and AChE, respectively, moved back to the original positions with root mean square deviations (RMSD) accounting for all the heavy atoms equal to 0.762, 0.390, and 0.147 Å, respectively (Figure S1).

Docking scores for **ABH2**, **ABH3**, and **ABH5** over the three biological targets MAO-A, MAO-B, and AChE are provided in Table 3. The values of **ABH5** were the best for the three enzymes.

https://dx.doi.org/10.1021/acscombsci.0c00136
ACS Comb. Sci. XXXX, XXX, XXX−XXX

Table 3. Docking scores for ABH2, ABH3, and ABH5 toward MAO-A, MAO-B, and AChE

compounds	docking scores (kcal/mol)		
	MAO-A	MAO-B	AChE
ABH2	−7.429	−8.929	−7.690
ABH3	−7.545	−8.427	−7.570
ABH5	−7.621	−9.430	−8.934

In Figure 4, a similar posing was observed for the binding modes of **ABH3**, **ABH2**, and **ABH5** to MAO-A. In particular, *para*-chloro phenyl of **ABH3** and **ABH5** faced FAD, formed $\pi-\pi$ interactions with the side chain of Y407 at a distance between the centroids of aromatic rings equal to 4.15 and 3.87 Å, respectively, and lied almost parallel in front of the aromatic ring of Y444. On the other hand, the *para*-fluoro benzyl of **ABH2** behaved similarly by substantially participating the same interactions as those for **ABH3** and **ABH5**. In addition, $\pi-\pi$ T-shaped[33] interactions were also engaged by the three inhibitors with the side chain of F208, a MAO-A selective residue, at a distance between the centroids of aromatic rings equal to 4.99, 5.10, and 4.81 Å for **ABH2**, **ABH3**, and **ABH5**, respectively.

Interactions between **ABH3**, **ABH2**, and **ABH5** toward MAO-B were shown in Figure 5. The *para*-chloro benzyl of **ABH3**, the *para*-fluoro benzyl of **ABH2**, and the *para*-chloro phenyl of **ABH5** were engaged by aromatic interactions with Y398 (at a distance of 3.96 and 3.63 Å for **ABH2** and **ABH5**, respectively), Y435 (at a distance of 4.89 Å for **ABH3**), and FAD. Additionally, the three compounds shared $\pi-\pi$ T-shaped interactions with a MAO-B selective residue Y326, showing a distance equal to 4.97, 5.19, and 4.42 Å for **ABH2**, **ABH3**, and **ABH5**, respectively, and hydrophobic interactions with the side chain of I199, a MAO-B selective residue.

Interactions between AChE and the three compounds were shown in Figure 6. The *para*-chloro benzyl and *para*-chloro phenyl of **ABH3** formed $\pi-\pi$ interactions with Y341 (at a distance of 3.65 Å) and W286 (at a distance of 4.10 Å), respectively. **ABH2** engaged $\pi-\pi$ interactions between its *para*-fluoro benzyl and Y341 (at a distance of 4.07 Å), while **ABH5** made $\pi-\pi$ interactions with W86 (at a distance of 3.75 Å) through its benzyl group. Furthermore, the three ligands shared a hydrogen bond between ketohydrazone bridge and nitrogen atom of the backbone of F295 at a distance between HBD and HBA groups equal to 2.0, 2.5, and 1.6 Å for **ABH2**, **ABH3**, and **AHB5**, respectively.

For the sake of clarity, all the reported interactions were flagged by GLIDE, and each distance is within the standard range being maximum values equal to 2.7, 4.4, and 5.5 Å for HB, $\pi-\pi$ stacking, and T-shaped interactions, respectively.[33,34]

Molecular docking analyses of **ABH3**, **ABH2**, and **ABH5** with MAO-A, MAO-B and AChE provide a sound rationale for the observed activities. The highest IC_{50} values of the three ligands toward MAO-B were correlated well with the docking scores, for which $\pi-\pi$ interactions with Y326 were especially important. Most importantly, the overall best multitarget activity and the selectivity of **ABH5** for MAO-B were also consistent with the docking score values.

Our attention toward MAO-B was also supported by interrogation of ChEMBLdb, a large collection of 611,333 small molecules provided with high quality experimental bioactivity data.[35] MAO-B was near the top of the list generated by using our recently developed predictive platform MuSSel,[36,37] with the chemical structure of **ABH5** as a query. Results were provided in Supporting Information.

In the present study, synthesis of (hetero-)(arylidene)-arylhydrazide derivatives (**ABH1**−**ABH14**) and their evaluations for MAOs and AChE inhibitory activities were disclosed. Most of the compounds were effective toward MAO-B inhibition with low micromolar range potencies, and only few of them had moderate MAO-A inhibition. On the other hand, only two compounds (**ABH3** and **ABH5**) were shown AChE inhibition with moderate potencies. It is clear that compounds with 4-chlorophenyl hydrazide part is relatively more effective toward MAO-B inhibition than heteroayl part. Among the substituents used in series 2 (**ABH1**−**ABH6**), benzyloxy of **ABH5** could be considered as a good pharmacophore unit, exhibiting excellent inhibitory effects toward all the three enzymes with low IC_{50} values (MAO-A = 3.31 μM, MAO-B = 0.025 μM, and AChE = 16.5 μM). Kinetics and reversibility studies revealed that **ABH5** is a competitive and reversible type of MAO-B inhibitor. The study reveals that the arylidenephenylhydrazide with ether functionality (lead molecule **ABH5**)

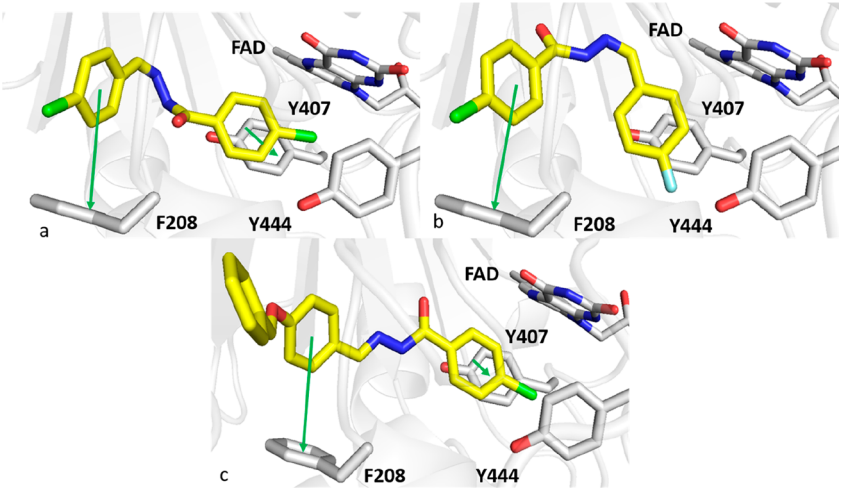

Figure 4. Panels a−c show the top-scored poses resulting from docking analyses of **ABH3**, **ABH2**, and **ABH5** toward MAO-A. Ligands and the target residues of the binding pocket are rendered in yellow and gray sticks, respectively. Green arrows indicate $\pi-\pi$ interactions.

https://dx.doi.org/10.1021/acscombsci.0c00136
ACS Comb. Sci. XXXX, XXX, XXX−XXX

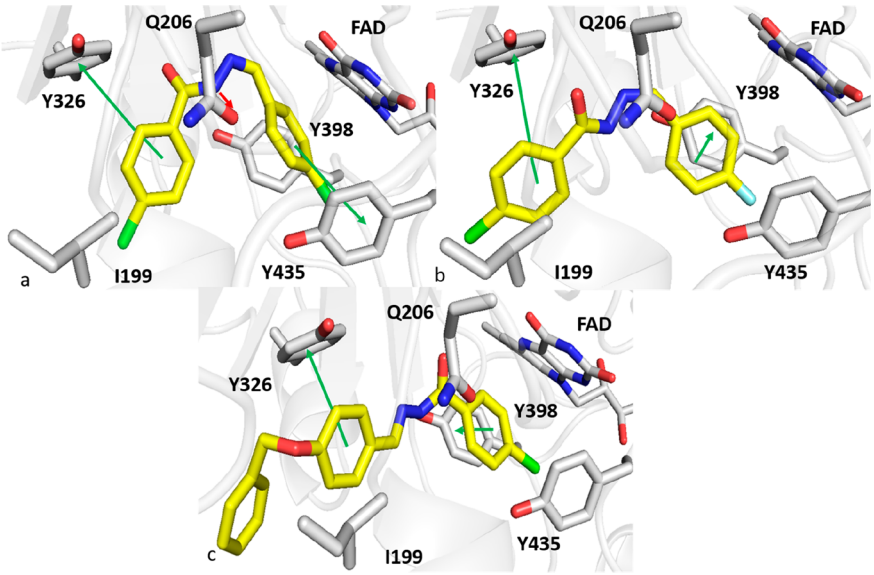

Figure 5. Panels a−c show the top scored poses resulting from docking analyses of **ABH3**, **ABH2**, and **ABH5** toward MAO-B. Ligands and the target residues of the binding pocket are rendered in yellow and gray sticks, respectively. Green and red arrows indicate $\pi-\pi$ interactions and hydrogen bonds, respectively.

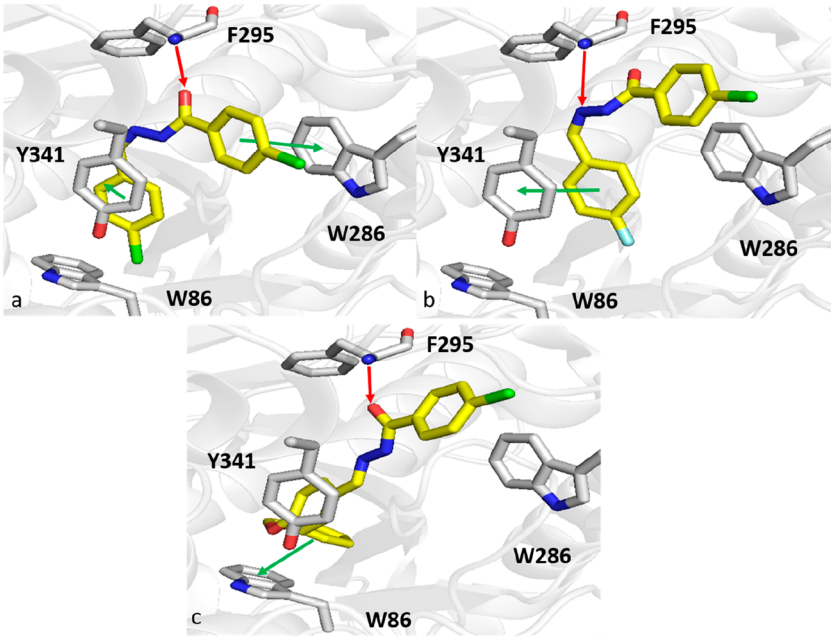

Figure 6. Panels a−c report the best poses resulting from docking analyses of **ABH3**, **ABH2**, and **ABH5** toward AChE. Ligands and the target residues of the binding pocket are depicted in yellow and gray sticks, respectively. Green and red arrows refer to $\pi-\pi$ interactions and hydrogen bonds, respectively.

may be considered as an emergent multitarget ligand in the interest of various neurodegenerative disorders.

■ ASSOCIATED CONTENT

Supporting Information

The Supporting Information is available free of charge at https://pubs.acs.org/doi/10.1021/acscombsci.0c00136.

Experimental procedures for synthesis of compounds, biochemical assay, and molecular docking and spectral characterization data (^{1}H NMR, ^{13}C NMR, and MS) for all the final compounds, along with spectra (PDF)

■ AUTHOR INFORMATION

Corresponding Authors

Hoon Kim − *Department of Pharmacy, and Research Institute of Life Pharmaceutical Sciences, Sunchon National University, Suncheon 57922, Republic of Korea;* orcid.org/0000-0002-7203-3712; Email: hoon@sunchon.ac.kr, hoon@scnu.ac.kr

Bijo Mathew − *Division of Drug Design and Medicinal Chemistry Research Lab, Department of Pharmaceutical Chemistry, Ahalia School of Pharmacy, Palakkad 678557, Kerala, India; Department of Pharmaceutical Chemistry, Amrita School of Pharmacy, Amrita Vishwa Vidyapeetham, Amrita Health Science Campus, Kochi 682 041, India;* orcid.org/0000-0002-6658-

https://dx.doi.org/10.1021/acscombsci.0c00136
ACS Comb. Sci. XXXX, XXX, XXX−XXX

4497; Email: bijovilaventgu@gmail.com, bijo.mathew@ahalia.ac.in

Authors

Ashique Palakkathondi − *Department of Pharmaceutical Chemistry, Al-Shifa College of Pharmacy, Perinthalmanna 679322, Kerala, India*

Jong Min Oh − *Department of Pharmacy, and Research Institute of Life Pharmaceutical Sciences, Sunchon National University, Suncheon 57922, Republic of Korea*

Sanal Dev − *Department of Pharmaceutical Chemistry, Al-Shifa College of Pharmacy, Perinthalmanna 679322, Kerala, India*

T. M. Rangarajan − *Department of Chemistry, Sri Venketeswara College, University of Delhi, New Delhi 110021, India;* orcid.org/0000-0002-5972-1879

Swafvan Kaipakasseri − *Department of Pharmaceutical Chemistry, Al-Shifa College of Pharmacy, Perinthalmanna 679322, Kerala, India*

Fathima Sahla Kavully − *Department of Pharmaceutical Chemistry, Al-Shifa College of Pharmacy, Perinthalmanna 679322, Kerala, India*

Nicola Gambacorta − *Dipartimento di Farmacia-Scienze del Farmaco, Università degli Studi di Bari "Aldo Moro", I-70125 Bari, Italy*

Orazio Nicolotti − *Dipartimento di Farmacia-Scienze del Farmaco, Università degli Studi di Bari "Aldo Moro", I-70125 Bari, Italy;* orcid.org/0000-0001-6533-5539

Complete contact information is available at: https://pubs.acs.org/10.1021/acscombsci.0c00136

Author Contributions

[#]A.P., J.M.O., and S.D. contributed equally to this work.

Notes

The authors declare no competing financial interest.

■ ACKNOWLEDGMENTS

This research was supported by the National Research Foundation of Korea (NRF) grant funded by the Republic of Korea government (NRF-2019R1A2C1088967) (to H.K.).

■ REFERENCES

(1) Harilal, S.; Jose, J.; Parambi, D. G. T.; Kumar, R.; Mathew, G. E.; Uddin, M. S.; Kim, H.; Mathew, B. Advancements in nanotherapeutics for Alzheimer's disease: Current perspectives. *J. Pharm. Pharmacol.* **2019**, *71*, 1370−1383.

(2) Kabir, M. T.; Uddin, M. S.; Begum, M. M.; Thangapandiyan, S.; Rahman, M. S.; Aleya, L.; Mathew, B.; Ahmed, M.; Ashraf, G. M.; Barreto, G. E. Cholinesterase inhibitors for alzheimer's disease: Multitargeting strategy based on anti-Alzheimer's drugs repositioning. *Curr. Pharm. Des.* **2019**, *25*, 3519−3535.

(3) Mathew, B.; Parambi, D. G. T.; Mathew, G. E.; Uddin, M. S.; Inasu, S. T.; Kim, H.; Marathakam, A.; Unnikrishnan, M. K.; Carradori, S. Emerging therapeutic potentials of dual-acting MAO and AChE inhibitors in Alzheimer's and Parkinson's diseases. *Arch. Pharm.* **2019**, *352*, e1900177.

(4) Carradori, S.; Silvestri, R. New frontiers in selective human MAO-B inhibitors. *J. Med. Chem.* **2015**, *58*, 6717−6732.

(5) Kim, D.; Baik, S. H.; Kang, S.; Cho, S. W.; Bae, J.; Cha, M. Y.; Sailor, M. J.; Inhee, M.-J.; Ahn, K. H. Close correlation of monoamine oxidase activity with progress of alzheimer's disease in mice, observed by in vivo two-photon imaging. *ACS Cent. Sci.* **2016**, *2*, 967−975.

(6) Legoabe, L.; Kruger, J.; Petzer, A.; Bergh, J. J.; Petzer, J. P. Monoamine oxidase inhibition by selected anilide derivatives. *Eur. J. Med. Chem.* **2011**, *46*, 5162−5174.

(7) Mathew, B.; Haridas, A.; Suresh, J.; Githa, E. M.; Ucar, G.; Jayaprakash, V. Monoamine oxidase inhibitory actions of chalcones. A mini review. *Cent. Nerv. Syst. Agents Med. Chem.* **2016**, *16*, 120−136.

(8) Mathew, B.; Haridas, A.; Uçar, G.; Baysal, I.; Adeniyi, A. A.; Soliman, M. E. S.; Joy, M.; Mathew, G. E.; Lakshmanan, B.; Jayaprakash, V. Exploration of chlorinated thienyl chalcones: A new class of monoamine oxidase-B inhibitors. *Int. J. Biol. Macromol.* **2016**, *91*, 680−695.

(9) Mathew, B.; Haridas, A.; Uçar, G.; Baysal, I.; Joy, M.; Mathew, G. E.; Lakshmanan, B.; Jayaprakash, V. Synthesis, biochemistry, and computational studies of brominated thienyl chalcones: A new class of reversible MAO-B inhibitors. *ChemMedChem* **2016**, *11*, 1161−1171.

(10) Shalaby, R.; Petzer, J. P.; Petzer, A.; Ashraf, U. M.; Atari, E.; Alasmari, F.; Kumarasamy, S.; Sari, Y.; Khalil, A. SAR and molecular mechanism studies of monoamine oxidase inhibition by selected chalcone analogs. *J. Enzyme Inhib. Med. Chem.* **2019**, *34*, 863−876.

(11) Reeta; Baek, S. C.; Lee, J. P.; Rangarajan, T. M.; Ayushee; Singh, R. P.; Singh, M.; Mangiatordi, G. F.; Nicolotti, O.; Kim, H.; Mathew, B. Ethyl acetohydroxamate incorporated chalcones: Unveiling a novel class of chalcones for multitarget monoamine oxidase-B inhibitors against Alzheimer's disease. *CNS Neurol. Disord.: Drug Targets* **2019**, *18*, 643−654.

(12) Oh, J. M.; Rangarajan, T. M.; Chaudhary, R.; Singh, R. P.; Singh, M.; Singh, R. P.; Tondo, A. R.; Gambacorta, N.; Nicolotti, O.; Mathew, B.; Kim, H. Novel class of chalcone oxime ethers as potent monoamine oxidase-B and acetylcholinesterase inhibitors. *Molecules* **2020**, *25*, 2356.

(13) Mathew, B.; Baek, S. C.; Thomas Parambi, D. G.; Lee, J. P.; Mathew, G. E.; Jayanthi, S.; Vinod, D.; Rapheal, C.; Devikrishna, V.; Kondarath, S. S.; Uddin, Md. S.; Kim, H. Potent and highly selective dual-targeting monoamine oxidase-B inhibitors: Fluorinated chalcones of morpholine versus imidazole. *Arch. Pharm.* **2019**, *352*, No. e1800309.

(14) Badavath, V. N.; Baysal, I.; Ucar, G.; Sinha, B. N.; Jayaprakash, V. Monoamine oxidase inhibitory activity of novel pyrazoline analogues: Curcumin based design and synthesis. *ACS Med. Chem. Lett.* **2016**, *7* (1), 56−61.

(15) Turan-Zitouni, G.; Hussein, W.; Saglık, B. N.; Tabbi, A.; Korkut, B. Design, synthesis and biological evaluation of novel N-pyridyl-hydrazone derivatives as potential monoamine oxidase (MAO) inhibitors. *Molecules* **2018**, *23*, 113−124.

(16) Can, N. O.; Osmaniye, D.; Levent, S.; Saglık, B. N.; Inci, B.; Ilgın, S.; Özkay, Y.; Kaplancıklı, Z. A. Synthesis of new hydrazone derivatives for MAO enzymes inhibitory activity. *Molecules* **2017**, *22*, 1381−1399.

(17) Hagenow, J.; Hagenow, S.; Grau, K.; Khanfar, M.; Hefke, L.; Proschak, E.; Stark, H. Reversible small molecule inhibitors of MAO A and MAO B with anilide motifs. *Drug Des., Dev. Ther.* **2020**, *14*, 371−393.

(18) Kavully, F. S.; Oh, J. M.; Dev, S.; Kaipakasseri, S.; Palakkathondi, A.; Vengamthodi, A.; Abdul Azeez, R. F.; Tondo, A. R.; Nicolotti, O.; Kim, H.; Bijo Mathew. Design of enamides as new selective monoamine oxidase-B inhibitors. *J. Pharm. Pharmacol.* **2020**, *72*, 916−926.

(19) Mathew, G. E.; Oh, J. M.; Mohan, K.; Tengli, A.; Mathew, B.; Kim, H. Development of methylthiosemicarbazones as new reversible monoamine oxidase-B inhibitors for the treatment of Parkinson's disease. *J. Biomol. Struct. Dyn.* **2020**, DOI: 10.1080/07391102.2020.1782266.

(20) Mathew, B.; Baek, S. C.; Grace Thomas Parambi, D.; Pil Lee, J.; Joy, M.; Annie Rilda, P. R.; Randev, R. V.; Nithyamol, P.; Vijayan, V.; Inasu, S. T.; Mathew, G. E.; Lohidakshan, K. K.; Kumar Krishnan, G.; Kim, H. Selected aryl thiosemicarbazones as a new class of multi-targeted monoamine oxidase inhibitors. *MedChemComm* **2018**, *9*, 1871−1881.

(21) Ellman, G. L.; Courtney, K. D.; Andres, V., Jr.; Feather-Stone, R. M. A new and rapid colorimetric determination of acetylcholinesterase activity. *Biochem. Pharmacol.* **1961**, *7*, 88−95.

(22) Baek, S. C.; Park, M. H.; Ryu, H. W.; Lee, J. P.; Kang, M. G.; Park, D.; Park, C. M.; Oh, S. R.; Kim, H. Rhamnocitrin isolated from *Prunus padus* var. seoulensis: A potent and selective reversible inhibitor of human monoamine oxidase A. *Bioorg. Chem.* **2019**, *83*, 317−325.

(23) Parambi, D. G. T.; Oh, J. M.; Baek, S. C.; Lee, J. P.; Tondo, A. R.; Nicolotti, O.; Kim, H.; Mathew, B. Design, synthesis and biological evaluation of oxygenated chalcones as potent and selective MAO-B inhibitors. *Bioorg. Chem.* **2019**, *93*, 103335.
(24) Son, S. Y.; Ma, J.; Kondou, Y.; Yoshimura, M.; Yamashita, E.; Tsukihara, T. Structure of human monoamine oxidase A at 2.2-A resolution: the control of opening the entry for substrates/inhibitors. *Proc. Natl. Acad. Sci. U. S. A.* **2008**, *105*, 5739−5744.
(25) Binda, C.; Wang, J.; Pisani, L.; Caccia, C.; Carotti, A.; Salvati, P.; Edmondson, D. E.; Mattevi, A. Structures of human monoamine oxidase B complexes with selective non-covalent inhibitors: safinamide and coumarin analogs. *J. Med. Chem.* **2007**, *50*, 5848−5852.
(26) Cheung, J.; Rudolph, M. J.; Burshteyn, F.; Cassidy, M. S.; Gary, E. N.; Love, J.; Franklin, M. C.; Height, J. J. Structures of human acetylcholinesterase in complex with pharmacologically important ligands. *J. Med. Chem.* **2012**, *55*, 10282−10286.
(27) Schrödinger. *Schrödinger Suite 2018-4 Protein Preparation Wizard*.
(28) Madhavi Sastry, G.; Adzhigirey, M.; Day, T.; Annabhimoju, R.; Sherman, W. Protein and Ligand Preparation: Parameters, Protocols, and Influence on Virtual Screening Enrichments. *J. Comput.-Aided Mol. Des.* **2013**, *27*, 221−234.
(29) Mangiatordi, G. F.; Alberga, D.; Pisani, L.; Gadaleta, D.; Trisciuzzi, D.; Farina, R.; Carotti, A.; Lattanzi, G.; Catto, M.; Nicolotti, O. A Rational Approach to Elucidate Human Monoamine Oxidase Molecular Selectivity. *Eur. J. Pharm. Sci.* **2017**, *101*, 90−99.
(30) *LigPrep*; Schrödinger, LLC.: New York, NY, 2018.
(31) Friesner, R. A.; Banks, J. L.; Murphy, R. B.; Halgren, T. A.; Klicic, J. J.; Mainz, D. T.; Repasky, M. P.; Knoll, E. H.; Shelley, M.; Perry, J. K.; Shaw, D. E.; Francis, P.; Shenkin, P. S. Glide: A New Approach for Rapid, Accurate Docking and Scoring. 1. Method and Assessment of Docking Accuracy. *J. Med. Chem.* **2004**, *47*, 1739−1749.
(32) Banks, J. L.; Beard, H. S.; Cao, Y.; Cho, A. E.; Damm, W.; Farid, R.; Felts, A. K.; Halgren, T. A.; Mainz, D. T.; Maple, J. R.; Murphy, R.; Philipp, D. M.; Repasky, M. P.; Zhang, L. Y.; Berne, B. J.; Friesner, R. A.; Gallicchio, E.; Levy, R. M. Integrated Modeling Program, Applied Chemical Theory (IMPACT). *J. Comput. Chem.* **2005**, *26*, 1752−1780.
(33) Sinnokrot, M. O.; Sherrill, C. D. Substituent Effects in $\pi-\pi$ Interactions: Sandwich and T-Shaped Configurations. *J. Am. Chem. Soc.* **2004**, *126*, 7690−7697.
(34) Herschlag, D.; Pinney, M. M. Hydrogen Bonds: Simple after All? *Biochemistry* **2018**, *57*, 3338−3352.
(35) Gaulton, A.; et al. The ChEMBL database in 2017. *Nucleic Acids Res.* **2017**, *45*, D945−D954.
(36) Montaruli, M.; Alberga, D.; Ciriaco, F.; Trisciuzzi, D.; Tondo, A. R.; Mangiatordi, G. F.; Nicolotti, O. Accelerating drug discovery by early protein drug target prediction based on multi-fingerprint similarity search. *Molecules* **2019**, *24*, 2233.
(37) Alberga, D.; Trisciuzzi, D.; Montaruli, M.; Leonetti, F.; Mangiatordi, G. F.; Nicolotti, O. A new approach for drug target and bioactivity prediction: the Multi-fingerprint Similarity Search aLgorithm (MuSSeL). *J. Chem. Inf. Model.* **2019**, *59*, 586−596.

https://dx.doi.org/10.1021/acscombsci.0c00136
ACS Comb. Sci. XXXX, XXX, XXX−XXX